Increased Association of Deamidated αA-N101D with Lens Membrane of Transgenic αAN101D vs. Wild Type αA Mice: Potential Effects on Intracellular Ionic Imbalance and Membrane Disorganization

Om Srivastava (srivasta@uab.edu)
Birmingham City University Kenrick Library https://orcid.org/0000-0001-5727-4801
Kiran Srivastava
University of Alabama at Birmingham
Roy Joseph
University of Alabama at Birmingham
Landon Wilson
University of Alabama at Birmingham

Research article

Keywords: Lens, Crystallins, Deamidation, Post-translational modifications, Transgenic Mice, Cataract.

Posted Date: November 27th, 2019

DOI: https://doi.org/10.21203/rs.2.17769/v1

Version of Record: A version of this preprint was published on December 10th, 2020. See the published version at https://doi.org/10.1186/s12886-020-01734-0.

Abstract

Background: We have generated mouse models by inserting the human lens αA-N101D transgene in CRYAAN101D mice, and human wild-type αA-transgene in CRYAAWT mice. The CRYAAN101D mice developed cortical cataract at about 7-months of age relative to CRYAAWT mice. The objective of the study was to determine the following relative changes in the lenses of CRYAAN101D- vs. CRYAAWT mice: age-related changes with specific emphasis on protein insolubilization, relative membrane-association of αAN101D vs. WTαA, and changes intracellular ionic imbalance and membrane organization. Methods: Lenses from CRYAAWT and CRYAAN101D mice were compared for an age-related protein insolubilization. The relative lens membrane-association of the αAN101D and WTαA in the two types of mice was determined by immunohistochemical-, immunogold-labeling-, and western blot analyses. The relative levels of membrane-binding of recombinant αAN101D and WTαA was determined by an in vitro assay, and the levels of intracellular Ca 2+ uptake and Na, K-ATPase mRNA were determined in the cultured epithelial cells of the two types lenses. Results: Compared to the lenses of CRYAAWT, the lenses of CRYAAN101D mice exhibited: (A) An increase in age-related protein insolubilization beginning at about 4-months of age. (B) A greater lens membrane-association of αAN101D relative to WTαA during immunogold-labeling- and western blot analyses, including relatively a greater membrane swelling in the CRYAAN101D lenses. . (C) During in vitro assay, the greater levels of binding αAN101D to membranes relative to WTαA was observed. (D) The 75% lower level of Na,K-ATPase mRNA but 1.5X greater Ca 2+ uptake were observed in cultured lens epithelial cells of CRYAAN101D than those of CRYAAWT mice. Conclusions: The results show that an increased lens membrane association of αAN101D relative WTαA in CRYAAN101D mice than CRYAAWT mice, which causes intracellular ionic imbalance, and in turn membrane swelling leading to cortical opacity.

Background

Although the cornea is the primary refractive tissue performing 70-80% of refraction of the eye, the major function of the lens is in accommodation and to partly help in the refraction. The lens accommodative function gradually diminishes with age and is almost completely lost at age of > 50 years. The lens transparency plays an important role in focusing light on to the retina, but this role is gradually lost as it develops age-related opacity. Several unique factors maintain lens transparency for up to > 60 year of our life time. These include: cellular homeostasis among only two types of cells (epithelial to fiber cells) [1], and an orderly terminal differentiation of epithelial to fiber cells with precise organelles loss [2], the unique interactions among crystallins [3] with almost no protein turnover [4], the specialized lens metabolism [5], specific interactions among α-crystallin and membrane [6], the precise maintenance of intracellular and extracellular ionic concentrations [7], the low levels of cellular water and oxygen in the inner cortex and nuclear regions [8], and a unique membrane lipid composition [9]. Alterations among some of these lens unique factors play direct or indirect roles in pathogenesis of cataracts (e.g., pediatric and age-related cataracts). However, additional cataract-causative factors are also identified, which include mutations in crystallins [10], oxidative insults of crystallins and the loss of redox balance of

glutathione [11], extensive truncations of α-, β-, and γ-crystallins [12-20], a variety of post-translational modifications with deamidation as being the most abundant one [21-25], and the loss of membrane integrity [7, 26, 27]. These factors individually or in combination also cause lens opacity through altered lens cellular structures and contents, ionic imbalance, increased water and oxygen levels, loss of natural interactions among crystallins, and crystallins' unfolding, their degradation and cross-linking.

The three primary types of age-related cataracts are nuclear sclerotic, cortical, and posterior subcapsular. Among these, the age-related nuclear sclerotic cataract that progresses slowly over many years, is the most common type and primarily caused by the hardening and yellowing of cellular contents in the center of the lens. The cortical cataract refers to clouding of the peripheral portion of the lens, which is due to creation of clefts (fissures) resulting in appearance as spokes of a wheel pointing from the lens outside edge toward the center. In the posterior subcapsular cataract, the opacity develops beneath the lens capsule.

Our focus in this study is the potential role of deamidated crystallins in the age-related cataractogenic mechanism in human lenses. Deamidation of Asn and Gln to Asp and Glu in crystallins, respectively, introduces negative charges, which is shown to alter their hydrophobicity, tertiary structures, and crystallin-crystallin interactions, and leads to aggregation and cross-linking [21-27]. Our results show that only deamidation of Asn localized at specific sites in crystallins (e.g., deamidation of N101 but not of N123 residues in αA-crystallin [24], and of N146 but not of N78 of αB-crystallin) exhibited the above-described effects [25]. To show the potential effects of deamidation *in vivo*, we have generated mouse models by inserting the human lens αA-N101D transgene in CRYAAN101D mice, and human lens wild-type αA-transgene in CRYAAWT mice (to act as a control). The CRYAAN101D mice developed cortical cataract at about 7-months of age relative to CRYAAWT mice [28, 29]. This model for the first time showed that *in vivo expression* of the deamidated αAN101D caused cortical lens opacity, which was due to the disruption of fiber cell structural integrity and protein insolubilization as aggregates [28]. The comparative RNA sequencing and Ingenuity Pathway Analyses (IPA) of lenses from 2- and 4-months old CRYAAN101D- and CRYAAWT mice showed that the genes belonging to cellular assembly, and organization, and cell cycle and apoptosis networks were altered in αAN101D lenses [29]. This was accompanied with several cellular defects in αAN101D lenses that included defective terminal differentiation (increased proliferation and decreased differentiation) of epithelial cells to fiber cells, and reduced fiber cells denucleation and expressions of Rho A and Na,K-ATPase (the major lens membrane-bound molecular transporter) [29]. The findings also suggested the potential role of lens intracellular ionic imbalance as the major reason for the development of cataract [29].

The above findings suggested that the altered intracellular ionic imbalance could be due to potential loss of membrane integrity that caused cortical opacity at about 7-months of age in the CRYAAN101D mouse model. Therefore, the focus of the present study was to determine whether an increased membrane-association of αAN101D potentially compromises membrane integrity, and causes an ionic imbalance and leads to cataract development. The results show that relative to CRYAAWT lenses, the CRYAAN101D lenses exhibit: (A) an increasing age-related protein insolublization of αAN101D beginning around 4-

months of age, including relatively greater presence of high molecular weight (HMW) proteins. (B) An increased association of αAN101D to membranes. (C) About 75% reduction in Na, K-ATPase mRNA levels, and the 1.5 X higher levels of Ca^{2+} uptake in cultured CRYAAN101D lens epithelial cells, and (D) Membranes swelling. Together, the results suggest that an increased association of αAN101D with the membrane leads to impaired Na,K-ATPase activity, which in turn causes ionic imbalance, membrane swelling, fiber cell disorganization and cortical cataract development.

Methods

Ethics Statement

All animal experiments were performed per protocols approved by the Institutional Animal Care and Use Committee (IACUC) of the University of Alabama at Birmingham (Protocol no. 130208393). Mice were housed in a pathogen-free environment at the facility of the University of Alabama at Birmingham.

Materials

Unless stated otherwise, the molecular biology-grade chemicals were purchased from Millipore-Sigma (St. Louis, MO, USA) or Fisher (Atlanta, GA, USA) companies. The polyclonal anti-human aquaporin-0 (AQP0) antibody was purchased from Alpha Diagnostics (San Antonio, TX, USA). Additional commercial sources of various chemicals and antibodies used in the study are described throughout the text.

Generation of Transgenic Mice

The mouse model that expresses a human αA-crystallin gene in which Asn-101 was replaced with Asp and is referred to as αAN101D-transgene. This model has been considered to be “deamidated” in this study, and the mice expressing αAN101D-transgene are referred to here as $CRYAA_{N101D}$ mice. The mouse models by inserting the human lens αA-N101D transgene in CRYAAN101D mice, and human wild-type αA-transgene in CRYAAWT mice were generated in Dr. Om Srivastava’s laboratory [28].The mouse lenses were extracted after the mice were euthanized using the CO_2 procedure as per approved by the Institutional Animal Care and Use Committee (IACUC) of the University of Alabama at Birmingham (Protocol no.130208393). Adult (2–3 months) wild type mice (C57Bl6) were obtained from the university breeding colony. Animals were kept under a 12/12 h light–dark cycle and had *ad libitum* access to food and water. We have used 3 mice from each group of CRYAAWT mice control and αAN101D mice.

Isolation of Water Soluble (WS)- and Water Insoluble (WI)-Proteins from Mouse Lenses The WS- and WI-protein fractions from lenses of desired ages of CRYAAWT- and CRYAAN101D mice were prepared as previously described by us [28]. All procedures were performed at 5°C unless specified otherwise. The lenses were removed under a dissecting microscope and placed in 5°C-cold buffer A (5 mM Tris-HCl, 1 mM EDTA, 1 mM DTT, pH 7.8, and protease inhibitor cocktail [Roche Life Science, Indianapolis, IN]), and

centrifuged at 14,000 x g for 15 min at 5°C to separate the WS- and WI- protein fractions. The supernatant (WS-protein fraction) was collected, and the pellet (WI-protein fraction) was resuspended in buffer A, centrifuged as above. The recovery of WS- and WI-protein fractions was repeated twice, and the WS supernatants after each centrifugation steps were pooled. The final WI-protein pellet was solubilized in 5 mM Tris-HCl, pH 7.5, containing 4 M urea, 5 mM EDTA, and 5 mM EGTA. The protein concentrations in these fractions were determined by using a kit (Pierce Biotechnology-Thermo Fisher) using bovine serum albumin as a standard.

Membrane Isolation from Mouse Lenses

The membranes from lenses of 1- and 6-month-old CRYAAWT and CRYAAN101D mice were prepared as described previously [30, 31]. Lenses of identical ages from both types of mice were homogenized in buffer B (0.05 M Tris-HCl, pH 8.0 containing 5 mM EDTA, 1 mM DTT, 150 mM NaCl, and protease inhibitor cocktail [Roche, Indianapolis, IN]), and the preparations were centrifuged at 100,000 x g for 30 min using Beckman TL 100 centrifuge with a TLA 100.3 rotor. The supernatant was collected, and the pellets were washed twice with the above buffer B and centrifuged as above. This was followed by three additional washes with buffer B containing 8 M urea and centrifugation as above after each wash. Next, the pellet was washed twice with water and centrifuged as above. The pellet was then washed with 0.1 M cold (5^0C) NaOH [30, 31]. A final wash followed this with water and centrifugation as above to recover the purified lens membrane preparations as pellets.

Miscellaneous Methods

Mass Spectrometric Analysis

The mass spectrometric analysis was carried out at the Targeted Metabolomics and Proteomics Laboratory of the University of Alabama at Birmingham.

(A) In-Gel Digestion, NanocHiPLC-Tandem Mass Spectrometry, and Protein Pilot 4.5 Search Queries

Following SDS-PAGE analysis, the desired gel bands were excised, and an overnight wash removed the excess stain with 50% of 100 mM ammonium bicarbonate/50% acetonitrile. Next, the disulfide bonds were reduced by 25 mM dithiothreitol at 50^oC for 30 min, and the alkylation of the free thiols groups was carried out with 55 mM iodoacetamide for 30 min in the dark. The excess alkylating agent was removed and the gel pieces were washed twice with a 100 mM ammonium bicarbonate for 30 min, and was evaporated to dryness in a SpeedVac (Savant, ThermoFisher Scientific, Atlanta, GA) before the addition of 12.5 ng/µl of trypsin (Promega Gold Mass Spectrometry Grade, Madison, WI), and incubated overnight at 37oC. Peptides were extracted twice for 15 min from the gel pieces using a 1:1 mixture of 1% formic acid

and acetonitrile, then the extracts were and evaporated to dryness, and the samples were resuspended in 30 µl of a 0.1% formic acid before mass spectrometric analysis.

An aliquot (5 µL) of each digest was loaded onto a Nano cHiPLC 200 µm x 0.5 mm ChromXP C18-CL 3 µm 120Å reverse-phase trap cartridge (Eksigent, Dublin, CA) at 2 µL/min using an Eksigent autosampler (Eksigent, Dublin, CA). After washing the cartridge for 4 min with 0.1% formic acid in ddH20, the bound peptides were flushed onto a Nano cHiPLC column [200 µm x 15 cm. ChromXP C18-CL 3 µm 120Å] with a 45 min linear (5-50%) acetonitrile gradient in 0.1% formic acid at 1000 µl/min using an Eksigent Nano1D+LC (Eksigent, Dublin, CA). The column was washed with 90% acetonitrile-0.1% formic acid for 10 min and then re-equilibrated with 5% acetonitrile-0.1% formic acid for 10 min. The SCIEX 5600 Triple-TOF mass spectrometer (AB-Sciex, Toronto, Canada) was used to analyze the protein digest. The IonSpray voltage was 2300 V, and the declustering potential was 80 V. Ion spray, and curtain gases were set at 10 psi and 25 psi, respectively, and the interface heater temperature was 120^{o}C. Eluted peptides were subjected to a time-of-flight survey scan from 400-1250 m/z to determine the top twenty most intense ions for MS/MS analysis. Product ion time-of-flight scans at 50 msec were carried out to obtain the tandem mass spectra of the selected parent ions over the range from *m/z* 100-1500. Spectra are centroided and de-isotoped by Analyst software, version TF (Applied Biosystems). A β-galactosidase-trypsin digest was used to confirm the mass accuracy of the mass spectrometer. The tandem mass spectrometry data were processed to provide protein identifications using an in-house Protein Pilot 4.5 search engine (SCIEX) using the Mus musculus (Mouse) UniProt protein database and using a trypsin digestion parameter. All proteins that had at least one peptide with a confidence score of 95% or higher were considered as potential candidates**.**

(B) In-Solution Digestion Protocol for Mass Spectrometric Analysis

All of the reagents used were freshly prepared before their use. A 100-µL aliquot of the protein sample (1 mg) in 100 mM Tris buffer (pH 7.8) containing the 6M urea was mixed with the reducing reagent (DTT) and incubated for 1 h at room temperature. Next, 20 µL of the alkylating reagent (iodoacetamide) was added and incubated for 1 h at room temperature, and then 20 *µ*L of the reducing agent was added to consume any unreacted iodoacetamide and allowed to stand at room temperature for 1 h. The urea concentration was reduced to ~0.6 M by diluting the reaction mixture with 775 µL of water, 100-µL trypsin solution (20 µg of stock trypsin) was added to bring protease-to-substrate ration 1-to-50, and the digestion was carried out overnight at 37°C. The trypsin digestion was stopped by adjusting the pH to <6.0 by adding concentrated acetic acid. The digest was analyzed directly or concentrated by evaporation. As needed, the samples were desalted using a C18 ZipTip™ (Millipore Corporation, Bedford, MA) using manufacturer's instructions. The mass spectrometric analysis was carried out as described above.

Purification of Recombinant WTaA- and aA-N101D-crystallins, their Conjugation with Alexa Fluor 350 and Membrane Binding

The WT aA- and aA-N101D mutant proteins were expressed in *E.coli* and purified by a Ni-affinity column chromatographic method as previously described by us [28]. Each protein was labeled with Alexa-350 using a protein labeling kit as suggested by the manufacturer (Molecular Probes, Carlsbad, CA).The binding of Alexa 350-conjugated WT aA- and aA-N101D mutant proteins to mouse lens membrane (isolated from C57 non-transgenic mice) was determined as previously described [32, 33]. During the binding assay, the purified lens membrane (containing 2.5 mg protein; isolated from 1 to 3-month old non-transgenic C57 mice) was incubated with increasing but identical concentrations of either Alexa-labelled WT aA- or aA-N101D proteins at 37^{o}C for 6 h. Next, the incubated preparations were centrifuged at 14,000Xg and the supernatant and pellet (membrane fraction) recovered. After washing the membrane fraction with water and centrifugation as above, the relative fluorescence of membranes incubated with WT aA- and aA-N101D mutant proteins was determined using Perkin Elmer Multiplate Reader (Model Victor1420-04).

Determination of Intracellular Ca^{2+} in Epithelial Cells in Culture from Lenses of CRYAAWT- and CRYAAN101D Mice

To culture epithelial cells, six 5-months old lenses from CRYAAWT- and CRYAAN101D mice were excised and incubated with 0.25% trypsin at 37^{o} C for 2.5 h in an incubator with 5% CO_2-humidified air. Next, the lens cells in trypsin solution were centrifuged at 1200 rpm for 3 min, and trypsin (in the supernatant) was discarded. The lens epithelial cells (recovered as pellet) were suspended in medium 199 (ThermoFisher Scientific, Grand Island, NY) containing 10% fetal calf serum (Hyclone, Logan, Utah) and 1% antibiotic-antimycotic solution (Thermo Fisher Scientific, Grand Island, NY) in 12-well plates (Corning, Franklin Lakes, NJ). After 24 h, the unattached cells were discarded by washing with the above medium. The old medium was replaced with fresh medium after every 48 h, and the cells were allowed to grow for 7 to 10 days until confluent. Next, the confluent cells were trypsinized and seeded in 12-well plates for intercellular Ca^{2+} determination and were allowed to grow for 24 h. The cells were washed with medium 199 without phenol red, incubated in calcium orange dye (Thermo Fisher Scientific, Grand Island, NY) at a final concentration of 4 μM for 30 min at room temperature as instructed in the manufacturer's protocol. After 30 min, the cells were washed with the above medium, and Ca^{2+} indicator was examined under a microscope (Leica DMI 4000B) using a Texas Red filter.

Western Blot and Immunohistochemical Analyses

The WS- and WI-proteins and membrane fractions isolated from lenses were analyzed for their immunoreactivity with anti-aquaporin 0 antibody (to visualize the membrane intrinsic protein), and anti-His monoclonal antibody ([Novagen, Madison, WI], to visualize WTαA and αAN101D) during Western blot

analysis. The SDS-PAGE analysis was carried out as described by Laemmli [34]. Confocal immunohistochemical analysis of lens axial sections was carried out as previously described by us [28]. The analysis was performed at the High-Resolution Imaging core facility of the University of Alabama at Birmingham.

Localization by Immunohistochemical-Transmission Electron Microscopic Method

The analysis was performed at the High-Resolution Imaging core facility of the University of Alabama at Birmingham. The His-tagged αA-WT- and αA-N101D-crystallins were localized in lens cells by an immunogold method. Lenses of desired ages were fixed in phosphate-buffered saline, pH 7.4 containing 4% paraformaldehyde and 0.05% glutaraldehyde (Electron Microscopy Sciences, Hatfield, PA) for 2 h at room temperature, and then overnight at 4°C. The fixed lenses were washed with water (Millipore, Billerica, MA). Samples were dehydrated by ascending ethanol gradient series followed by infiltration overnight at 4°C with absolute ethanol: London Resin (LR) white (1:1). Next, the samples were incubated overnight with pure LR white resin on a rotating platform. The lenses were removed and transferred to gelatin capsules containing fresh LR white and allowed to polymerize for 24 h at 45-50°C. Ultra-thin (silver gold to light gold) LR white lens sections were collected on nickel mesh grids. The color of sections was silver-gold to light gold, and based on their color, the thickness was estimated to between 70-80 nm. For immunogold-labeling, the protocol as described in Electron Microscopy Sciences (Hatfield, PA) was precisely followed. To inactivate aldehyde groups present after aldehyde fixation, the samples on grids were incubated on 0.05 M glycine in PBS buffer for 10-20 minutes. Next, the grids were transferred onto drops of the matching Aurion blocking solution for 15 min, and then were washed for 15 min in incubation solution (PBS containing 0.1% bovine serum albumin and 15 mM NaN3, pH 7.3). This was followed by a 2X wash in incubation buffer, each time for 5 min. The grids were incubated with two primary antibodies (anti-His monoclonal antibody [10 nm diameter] and anti-aquaporin 0 polyclonal antibody [25 nm diameter]) for 1 h. In controls, the primary antibodies were omitted. The grids were then washed 6X (5 minutes each time) with the incubation solution and transferred to drops of the appropriate gold conjugate reagent, diluted 1/20-1/40 in the incubation solution for 30 minutes to 2 h. The grids were washed on drops of incubation solution for 6X (5 min each time). The grids were washed twice with PBS for 5 min, post-fixed in 2% glutaraldehyde in PBS for 5 min, and finally washed with distilled water and contrasted according to standard procedures. Lens sections were imaged using an FEI 120kv Spirit TEM (FEI-ThermoFisher), and images were collected using an AMT (AMT-Woburn, MA) digital camera.

RNA Extraction and Reverse Transcription-Quantitative Polymerase Chain Reaction (RT-PCR [qPCR])

RNA was extracted with Trizol reagent (Invitrogen) from cultured lens epithelial cells from CRYAAN101D and CRYAAWT mice, and all the samples were analyzed in triplicates. Real-time PCR quantifications were performed using the BIO-RAD iCycler iQ system (Bio-Rad, Hercules, CA), using a 96-well reaction plate for

a total volume of 25 µL. RNA was extracted as described above. Primers were designed using Primer3 for the following genes:

Atp1a2 Forward-5'CGGGAGCCATAAGGGTTTGT 3', and **Atp1a2** Reverse- 5'GCACTGACTTGGCTGTTGTG 3'

The ACTB gene was used for normalization. The reaction mixture included 12.5 µL of Real- Time SYBR Green PCR master mix, 2.5 µL of reverse transcription product, 1 µL of forward and reverse primer and 8 µL of DNase/RNase free water. The reaction mixtures were initially heated to 95ºC for 10 min to activate the polymerase, followed by 40 cycles, which consisted of a denaturation step at 95ºC for 15 sec, annealing at 55ºC for 60 sec and an elongation step at 72ºC. The qRT-PCR data were analyzed by the comparative ΔCt method.

Results

Age-Related Protein Insolubilization in Lenses of CRYAAN101D and CRYAAWT Mice

The WS- and WI-protein fractions were isolated from two lenses of CRYAAN101D and CRYAAWT mice of ages of 1-, 3-, 4-, 5- and 7-months, and their protein profiles were compared by SDS-PAGE analysis. To normalize comparison among WS-and WI-protein profiles of the lenses of the mice of different ages, the lenses from each age mice were identically processed using identical volumes of buffers to recover their WS- and WI-proteins. Further, an equal volume of WS- or WI-proteins preparations from lenses of each ages of the two types of mice were used during the SDS-PAGE analysis. These normalizing steps allowed the comparative determination of profiles of age-related changes in the WS- and WI-proteins of the lenses. The comparative WS-protein profiles from the lenses of the CRYAAN101D (identified as transgenic in Fig.1) and CRYAAWT (identified as WT in Fig. 1) mice were almost identical up to 3-months of age. However, the WI-protein preparations from CRYAAN101D mice of 4-, 5- and 7-months showed relatively higher levels of proteins, which included levels of crystallins (M_r between 20-35 kDa) and their aggregated species (M_r > 45 kDa) in the αAN101D lenses relative to wild-type lenses beginning at 4-months of age (Lanes 4 and 5 in Fig 1B). This suggested that the increasing levels of WS-proteins showed age-related water-insolubilization beginning at 4-months of age in the lenses of αAN101D mice (see Table in Figure 1). Between 4- to 7-months of age, about 5 to 10% higher proteins became water insoluble in lenses of CRYAAN101D relative to lenses of WT mice. To determine changes in individual crystallins due to their insolublization, the WS-protein fraction from 7-month-old lenses was fractionated by a size-exclusion HPLC using a G-4000PWXL column (Tosoh Biosciences, fractionation range of protein with M_r's between $1X10^4$ to $1X10^7$ kDa). The comparative protein elution profiles at 280 nm of 7-month old lenses of CRYAAWT and CRYAAN101D mice showed an increased protein in the void volume peak (representing WS-HMW proteins), and reduced β- and γ-crystallin peaks in the latter (differences shown in green in Figure 2A). The void volume peak in WS-protein fraction was also higher in the 7-month old lenses relative to 1-month old lenses of CRYAAN101D mice (Results not shown), suggesting an increased HMW protein aggregate formation with aging. On western blot analysis of the individual column fractions nos. 6 to 9 (constituting the void volume-HMW-protein peak) with an anti-His antibody, the His-

immunoreactive protein levels were higher in 7-month old CRYAAN101D lenses compared to the identical aged CRYAAWT lenses (Figure 2B). Additionally, the immunoreactive peak in the WT lenses was in the fractions no. 8 and 9 whereas it was in the fractions no. 7 and 8 in the αAN101D lenses, suggesting that the HMW proteins of αAN101D lenses had a higher molecular weight relative to the HMW proteins from WTαA lenses. On quantification with Image J, the intensity of the immunoreactive HMW proteins of αAN101D was about 20% greater relative to WTαA-lenses. Together, the results suggested a greater aggregation with higher M_r of the HMW-protein fraction in αAN101D lenses relative to WTαA lenses.

Identification Proteins Present in Water Insoluble-Urea Soluble (WI-US) - and Water Insoluble Urea Insoluble (WI-UI) Protein Fractions of Lenses of CRYAAWT and CRYAAN101D Mice

To Identify the insolubilized proteins in WTαA vs. αAN101D lenses, the WI-proteins from 5-month-old mice were further fractionated into WI-US- and WI-UI-protein fractions, examined by SDS-PAGE (Figure 3), which was followed by mass spectrometric analysis to determine their protein compositions. SDS-PAGE analysis showed that both WI-US- and WI-UI-fractions from CRYAAN101D lenses contained greater levels of proteins including aggregated proteins (M_r > 30 kDa) [Identified as a and c in Figure 3] relative to the same fractions from lenses of CRYAAWT mice (Identified as b and d in Figure 3). The mass spectrometric analysis was carried out at the following two levels: (i) In the first level analysis, determination of the total protein compositions in the WI-US- and WI-UI protein fractions of the two types of lenses (Supplemental (A) Tables 1 [Comparative protein compositions of WI-US-fractions of αAN101D and WTαA lenses], and Supplemental (B) Table 2 [Comparative protein compositions of WI-UI-fractions of αAN101D and WTαA lenses]). (ii) In the second level analysis, the protein compositions of aggregates (M_r >30 kDa) in WI-US-protein fraction of αAN101D lenses (Identified as ‘a’ in Figure 3), and WI-US-protein fraction of WTαA lenses (Identified as ‘b’ in Figure 3) [Supplemental (C) Table 3]. Similarly, the compositions of protein aggregates (M_r >30 kDa) in WI-UI-fraction of αAN101D lenses (Identified as ‘c’ in Figure 3,), and WI-US-fraction of WTαA lenses (Identified as ‘d' Figure 3) were determined [Supplemental (D) Table 4]. The rationale of the two levels of analysis was to determine the relative proteins compositions due to the greater insolublization of proteins in CRYAAN101D lenses relative to CRYAAWT lenses (Figure 1, Table1). The level 1 determination was expected to identify the total proteins that showed insolubilization and existed in the US- and UI-protein fractions, whereas the level 2 analysis was intended to selectively identify those proteins that formed aggregates in the US- and UI-fractions. The expectation was that the information from the analyses would implicate role of specific crystallins in the aggregation and in the cataractogenic mechanism.

(i) Comparative Protein Compositions in WI-US Fractions of Lenses from CRYAAN101D and CRYYAAWT Mice

The proteins detected in the WI-US-protein fractions of CRYAAN101D lenses but were absent in the CRYYAAWT lenses were [described in Supplemental (A) Table 1]: α-enolase, ATP synthase subunit beta (mitochondrial), several histones (H1.1, H1.2, H1.3, H1.4, H2B type 1-A, H2B type 1-B, H2B type 1-C, H2B type 1-F/J/L, H2B type 1- H2B type 1-H, H2B type 1-K, H2B type 1-M, H2B type 1-P, H2B type 2B, H2B type 2E, H2B type 3A, H2B type 3B, H3.1, H3.2, H3.3, H3.3C, H4), and keratin type 1 and 2 (cytoskeleton). In contrast, the CRYYAAWT lenses contained the following proteins that were absent in the CRYAAN101D lenses (Supplemental Table 1): ezrin, gamma crystallin N, histones (2A type 1, H2A.V, H2A.Z, H2A.X), lengsin, moesin, N6- adenosine-methyltransferase subunit METTL3, pyruvate kinase PKM, radixin, retinal dehydrogenase, spectrin beta chain (non-erythrocytes), and tubulin with alpha-1A and alpha 3 chains. Together, the above results show that the WI-US fraction of CRYAAN101D lenses was enriched in several histones, which could be due to the lack of denucleation relative to CRYYAAWT lenses. Furthermore, the insolubilized proteins that could be solubilized in 8M urea from the two types of lenses were different.

(ii) Comparative Protein Compositions of WI-UI-Fractions of Lenses from CRYAAN101D- and CRYYAAWT Mice

On a comparison of the proteins present in the WI-UI-protein fractions of CRYAAN101D lenses but were absent in CRYYAAWT lenses, these were [Supplemental (B) Table 2]: ATP synthase subunit alpha and beta (mitochondrial), Cadherin-2, histones (H1.0, 1.2, 1.3, 1.4, H2A-type 1, H2A-type1-H-F, H2A-type 1-H, H2A-type 1-K, H2A type2-A, H2A type2-C, H2A type 3, H2A.J, H2AX, H2B type 1-A, H2B type 1-B, H2B type 1-C/E/G, H2B type 1-F/J/L, H2B type 1-H, H2B type 1-K, H2B type 1-M, H2B type 1-P, H2-B type 2-B, H2-B type 2-E, H2B type 3-A, H2B type 3-B, H4), keratin type II and type 6 (cytoskeletal 2 epidermal), and N6-adenosine-methyltransferase subunit METTL3. In contrast, the CRYYAAWT lenses contained the following proteins that were absent in the CRYAAN101D lenses: (Supplemental Table 2): AFG3-like protein 2, ankyrin-2, armadillo repeat protein deleted in velo-cardio-facial syndrome homolog, catenin beta-1, elongation factor 2, γD-crystallin, gap junction alpha-8 protein, glyceraldehyde-3- phosphate dehydrogenase, guanine nucleotide-binding protein [G (i) subunit alpha-1, -subunit (i) alpha-2, -G(k) subunit alpha, -G(o) subunit alpha, -G (olf) subunit alpha, -G(s) subunit alpha, -G(s) subunit alpha isoform short, -G(s) subunit alpha XLas, -G(s) subunit alpha-1, -G(s) subunit alpha-2, -G(s) subunit alpha-3, G(s) subunit alpha-12, G(s) subunit alpha-13], heat shock 70 kDa protein-1A, -1B, -1-like, heat shock cognate 71 kDa protein, histone H4, importin 5, keratin, type I cytoskeletal 13, keratin, type I cytoskeletal 19, keratin, type II cytoskeletal 71, keratin, type II cytoskeletal 72, lens epithelial cell protein LEP503, multifunctional protein ADE2, peroxiredoxin-2, phosphoglycerate kinase, pyruvate kinase PKM, Rab GDP dissociation inhibitor beta, Ras-related C3 botulinum toxin substrate 1, Ras-related C3 botulinum toxin substrate 2, Ras-related C3 botulinum toxin substrate 3, Ras-binding protein 6, retinal dehydrogenase, tubulin (alpha-1A chain, -alpha-1C chain, -beta-2A chain, - beta-2B chain, - beta-4A chain, -beta-4B chain, -beta -5A chain), and ubiquitin carboxyl-terminal hydrolase isozyme. These results again show that the majority of histones that existed in CRYAAN101D lenses were absent in the CRYYAAWT lenses, which could be due to the lack of denucleation in the former lenses. Additionally, among crystallins, specifically αB and βB2

crystallin became insoluble as their levels were higher even in the WI-UI-fraction of CRYAAN101D lenses relative to CRYYAAWT lenses.

(iii) Compositions of Aggregated Proteins (M_r >30 kDa) in WI-US- and WI-UI-Fractions of Lenses from CRYAAN101D and CRYYAAWT Mice

As noted above, the purpose of the second level of mass spectrometric analysis was to elucidate the comparative compositions of aggregated proteins (M_r >30 kDa) in WI-US- and WI-UI-protein fractions of CRYAAN101D and CRYYAAWT lenses [Supplemental (C) and (D) Tables 3 and 4]. On comparison, the proteins present as aggregates (M_r > 30 kDa) in WI-US fraction of CRYAAN101D but absent in CRYYAAWT were (Table 3): basement membrane-specific heparin sulfate proteoglycan core protein, βB3- and γC-crystallins, calcium-uptake protein 2, (mitochondrial), collagen alpha-1(IV) chain and -alpha-2(IV) chain, glial fibrillary acidic protein and nestin. In contrast, the exclusively present proteins in WI-US fraction of CRYYAAWT were: N6-adenosine-methyltransferase subunit METTL3, and γC-, γD, γE- γF-crystallins. The above list describes the selective proteins that were water insoluble-urea soluble and became part of the complexes with M_r > 30 kDa in CRYAAN101D lenses. Because the aggregated proteins contained collagen, proteoglycans, and βB3- and γC-crystallins, and calcium uptake protein 2, (mitochondrial) in the WI-US fraction of αAN101D, we hypothesize relative cellular disorganization occurred in the CRYAAN101D lenses. Similarly, the greater abundance of αA- and βB1-crystallins in the aggregated form suggested their involvement in the aggregation process along with βB3- and γC-crystallins.

On comparison of proteins that existed in WI-UI protein fraction as > 30 kDa aggregates in but in CRYAAN101D not in the CRYYAAWT were [Supplemental (D) Table 4]: γB-, γD- and γE-crystallins, N6-adenosine-methyltransferase subunit METTL3, nestin, tail-anchored protein insertion receptor WRB. In contrast, on a comparison, the proteins as >30 kDa aggregates present in the WI-UI fraction of CRYYAAWT lenses but absent in CRYAAN101D lenses were: serine/arginine repetitive matrix protein 2. In the WI-UI fraction, the greater abundance of proteins in CRYAAN101D compared to CRYYAAWT were: αA-crystallin and lens fiber major intrinsic protein. Together, the results showed that the proteins that remained urea insoluble and were associated with the membrane of CRYAAN101D lenses were: γB-, γD- and γE-crystallins, and nestin. Nestin is an intermediate filament protein, which is expressed predominantly in the developing central nervous system and skeletal muscles.

Increased Association of αAN101D with Lens Membrane in the Outer Cortical Fiber Cells relative WTαA in CRYYAAWT lenses

Our previous report (28) showed an increased levels abnormal deposition of αAN101D within the outer cortical region in CRYAAN101D lenses compared WTαA in CRYYAAWT lenses, it suggested possible

relatively greater membrane binding of αAN101D. This was further investigated in experiments as described below.

(i) Immunohistochemical Analyses of Lenses from CRYAAN101D and CRYAAWT Mice

The purpose of the experiments was to determine relative levels of αAN101D and WTαA in the outer cortical regions of CRYAAN101D- vs.CRYAAWT lenses. This was examined by immunohistochemical analysis of 5-months old lenses of the two types of mice using anti-His monoclonal (for WTaA and aAN101D detection [green fluorescence])- and polyclonal anti-aquaporin 0 (for membrane detection [red fluorescence])-antibodies (Figure 4). The axial sections (at 10X magnification) showed an irregular and greater deposition of His-tagged aA (Green) in the lens outer cortex of CRYAAN101D mice (Shown by an arrow in Figure 4A) relative to CRYAAWT mice (Shown by an arrow in Figure 4B). Similarly, the equatorial sections (at 40X magnification) also exhibited a greater immunoreactive green fluorescence in the outer cortex of the CRYAAN101D lens relative to the CRYAAWT lens (shown by arrows in Figure 4C and D). Together, the results suggested the abnormally greater levels of association of αAN101D in the outer cortical regions and potentially with the fiber cell membranes in the CRYAAN101D lenses relative to those of CRYAAWT lenses.

(ii) Relative Membrane-Association of WTαA- and αA-N101D in Lenses of CRYAAN101D and CRYAAWT Mice

The rationale for the next experiment was that if greater membrane-association of αA-N101D occurs *in vivo* in CRYAAN101D lenses compared to CRYAAWT lenses, the difference in their levels could also be determined by western blot analysis in the purified membrane fractions isolated from the two types of lenses. The expectation was that following the step-wise membrane purification by using 8M urea (to dissociate non-covalently-bound membrane proteins), and by the final wash with 0.1N NaOH (to remove non-membranous extrinsic proteins) [30, 31], the relative levels of membrane-association of αAN101D vs. WTαA in the two types of lenses could be determined by the western blot analysis. To normalize the levels of the relative association during the membrane preparations, the two lenses of 1-month-old and two lenses from 6-month old from CRYAAN101D and CRYAAWT mice were identically processed using identical volumes of buffers at each steps during membrane purification (See Methods). Next, Western blot analysis using anti-His- and anti-aquaporin 0-antibodies were used to determine the relative levels of membrane-association of WTαA and αAN101D at different purification steps. To simplify the presentation of the western blot results of fractions recovered, during the steps of membrane purification, only the results of immunoblots with anti-His antibody but not with the western blot profiles with anti-aquaporin 0 are shown in Figure 5. However, the western blot profiles with anti-aquaporin 0 of the fractions were almost identical (Results not shown). The levels of His-tagged αA (green fluorescence) in lenses of 1-month old lenses (Figure 5, left panel: WTαA [A and C] and αAN101D [B and C]) and 6-month old lenses (Figure 5, right panel: WTαA [A and C] and αAN101D [B and D]) are shown. The upper (A) and (B) profiles in both left and right panels show Coomassie blue-stained protein bands, and the lower (C) and (D) show western blot immunoreactivity with the anti-His antibody. Additionally, in both left and right

upper panels, the lanes 1, 2 and 3 show the WS-protein fractions recovered after first, second and third consecutive washes in buffer A to solubilize WS-proteins, respectively. Lanes 4 and 5 represent the urea soluble-protein fractions recovered during two consecutive washes of WI-protein pellet (containing membranes) with buffer B containing 8M urea, respectively. Lane 6 represents the 0.1N NaOH-solubilized proteins from membranes and the lane 7 from both 1- and 6-month old lenses (left and right panels) show the purified lens membrane preparations. Similarly, lanes 7 and 8 from 6-month old lenses (right panel) represent purified membrane preparation. Lane 9 of 6-month old lenses represents crude WS-homogenate. The results show that the green fluorescence representing WTαA in CRYAAWT mice was entirely disappeared on urea solubilization in 1- and 6-month old lenses (lanes 1 to 5 in both left and right panels), whereas it was present in these lenses until 0.1N NaOH wash (lane 6 in left and right panels). In contrast, the green fluorescence still existed in lane 6 of membranes from 1- and 6-month old CRYAAN101D lenses. This suggests αAN101D was tightly bound and at the higher levels to lens membrane of CRYAAN101D lenses relative to CRYAAWT lenses.

On quantification of the Western blots using Image J (Figure 5, lower most panel), the lanes 4 and 5 (urea soluble fractions) of 1-month old lenses showed higher levels (2.5X) of immunoreactivity with anti-His antibody in the CRYAAN101D lenses (shown in red) compared to those from CRYAAWT lenses (blue). Similarly, among the lanes 4 and 5 containing same fractions from 6-month old lenses (as described in 1-month old lenses), the lane 5 showed a greater immunoreactive level of CRYAAN101D lenses (red) compared to CRYAAWT lenses (blue). Additionally, the lane 6 (representing membrane remaining after two urea washes, right panel) of 6-month CRYAAN101D lenses exhibited about 2X greater immunoreactivity than CRYAAWT lenses (Quantification results not shown). Together, the results show that relative to CRYAAWT, higher levels of CRYAAN101D were tightly associated with the lens membranes of 1- and 6- month old CRYAAN101D mice.

(iii) Relative Membrane-Binding of Alexa 350-Labeled Recombinant WTaA- and aA-N101D Crystallins

To examine whether aA-N101D show a greater binding affinity to the lens membrane relative to WTaA-crystallin, the binding of the two recombinant proteins to purified lens membrane was examined. The recombinant WT aA- and aA-N101D proteins were labeled with Alexa 350 using a protein labeling kit by the procedure described by the manufacturer (Molecular Probes, Thermofisher Scientific). The two labeled-proteins were purified by a size-exclusion HPLC column and were analyzed by SDS-PAGE. Figure 6A shows the Coomassie blue-stained WT aA (lane 1), aA-N101D protein (lane 2), and the purified lens membrane from non-transgenic C57 mice (lane 3). The Figure 6B shows the images of the two Alexa 35-labeled proteins under a UV trans-illuminator [Lane 1: Images of Alexa 350-labeled WTaA, and lane 2: Alexa 350-labeled aAN101D). During the binding assay, the purified lens membrane (containing 2.5 mg protein; isolated from 1 to 3-month old non-transgenic C57 mice) was incubated with increasing but identical concentrations of either Alexa-labelled WT aA- or aA-N101D proteins at 37^{o}C for 6 h (See details in Methods). A relatively higher levels (>1.5X) of binding of aAN101D proteins relative to WTaA with membrane preparation was observed

(Figure 6C). The values reported are the average of triplicate assays.

(iv) Immunogold-Labeling for Relative Localization of αA-WT and αA-N101D in Lens Membranes of CRAAN101D and CRAAWT Mice

To ascertain the relative levels association αAN101D vs. WTααA to the lens membrane *in vivo*, the immunogold-labeling experiment was carried out (See details in Methods). (A) and (B) in Figure 7 show lens membranes from CRYAAN101D and CRYAAWT at 500 nm magnification and (C) and (D) from these lenses at 100 nm magnification. The bigger gold particles (25 nm, red arrows) the smaller gold particles (10 nm, yellow arrows) represented the aquaporin 0 and the His-tagged αAN101D and WTαA, respectively. As shown in the representative images in (A) to (D), the 25 nm gold particles (representing aquaporin 0, identified by red arrows) were bound to membranes. On counting the membrane-associated 10 nm particles (representing His-tagged αAN101D and WTαA) almost the same numbers of the particle were found to be associated with membranes of both CRYAAN101D and CRYAAWT lenses, suggesting that the His-tagged αAN101D and WTαA were bound to the membranes of the two types of lenses. Our previous study [28] showed that αAN101D constituted about 14% and 14.2% of the total αA in the WS-and WI-proteins, respectively in the lenses of CRYAAN101d mice. Therefore, an argument can be made that although an almost equal number of 10 nm and 25 nm particles were associated with membranes of the two type of lenses, a higher number of gold particle representing αAN101D relative to WTαA were associated with the membrane.

Another interesting observation was that the membranes of CRYAAN101D lenses were about 2X more swollen relative to those of CRYAAWT lenses [Figure 7, compare (A) to (B) and (C) to (D)]. The swelling could represent water intake within the lens cells due to the potential ionic imbalance in the CRYAAN101D lenses compared to CRYAAWT lenses. Such a possibility of ionic imbalance was further determined as described below.

Na, K-ATPase and Ca^{2+} Levels in Cultured Epithelial Cells from Lenses of CRYAAN101D and CRYAAWT Mice

Sodium-potassium-adenosine triphosphatase (Na, K-ATPase) has been recognized for its role in regulating electrolyte concentrations in the lens, and the electrolyte balance is vital to lens transparency [35, 36]. In addition, calcium has been reported to control both sodium and potassium permeability through lens membranes [37]. In our previous study [29], we showed that the expression of Na,K-ATPase at the protein level was drastically reduced in CRYAAN101D lenses relative to CRYAAWT lenses. Next, the levels of Na, K-ATPase mRNA, and Ca2+ levels were determined in epithelial cells from lenses of CRYAAN101D and CRYAAWT mice. Both (A) and (B) in Figure 8 show intracellular Ca2+ levels in the presence of calcium orange in cultured epithelial cells from CRYAAN101D and CRYAAWT, respectively. Only a few CRYAAN101D cells showed the Ca2+ uptake, which was possibly due to our previous finding

that the lens cells contained only 14% of αAN101D mutant protein [28]. In this experiment, 100 cells from the two cultures were counted. On quantification by Image J of the number of cells that exhibited calcium orange uptake were 1.5X greater in CRYAAN101D lens cells relative to cells from CRYAAWT lenses (Figure 8B). On the determination of levels of mRNA of Na, K-ATPase in these cells, its level was 75% lower in the CRYAAN101D lens cells than CRYAAWT lens cells (Figure 9C).

Discussion

Several past studies have shown *in vitro* effects of deamidation of crystallins on their structural properties including those in αA- and αB-crystallins [21-25]. For example, deamidation of Q85 and Q180 in human βA3-crystallin decreased its heterodimer formation with βB1 or βB2-crystallins [35]. Similarly, *in vitro* studies also showed that deamidation of βA3 at Q42 and N54 in the N-terminal domain, at N133 and N155 in the C-terminal domain, and at N120 in the peptide connecting the N-terminal- and C-terminal domains, destabilized the crystallin's structure and caused aggregation in all the deamidated protein species [36]. Together, these reports suggest that deamidation might contribute to aggregation of lens crystallins *in vivo.*

No significant differences in the extent of deamidation in asparagine-101, glutamine-50, and glutamine-6 of αA-crystallin (purified from the nucleus of cataractous versus age-matched normal human lenses) was reported [40]. This study also showed no significant difference in the deamination at αAN101 site between cataractous- and age-matched non-cataractous human lenses even when this site was deamidated in both types of lenses. However, the deamidation at Gln-50 and Asn-101 positions in αA-crystallin was more frequent than Gln-6 and Asn-123, suggesting their higher susceptibility to *in vivo* deamidation [41]. The mass spectrometric analysis found that there is negligible (less than 1%) deamidation at αAN101 site in both aged and cataractous human lenses [42]. These studies suggested that because of low levels of deamidation of αA at N101 to D in normal and cataractous lenses, the αAN1010D might not play a significant role in cataract development. However, additional studies suggest otherwise. For example, our *in vitro* studies showed significant altered structural and functional properties of αA-crystallin on deamidation of N101 residue but not of N123 residue [24]. We also showed that the WS-protein fraction from 50-70 year old-human donors contained αA fragments with deamidation of N101 to D [43]. This finding is significant because recent studies have also shown an increasing role of crystallin fragments in cataract development [44, 45]. In the present study, the cortical cataract development in mice on the introduction of αA-N101D transgene further show significance of deamidation of this site and altered changes in the lens. However, the exact *in vivo* molecular mechanism of αA-N101D-induced crystallin's aggregation is yet to be fully understood.

Previously we showed that the three recombinant deamidated αA mutants (N101D, N123D, and N101D/N123D) exhibited reduced levels of chaperone activity, alterations in secondary and tertiary structures, and larger aggregates relative to WT-αA-crystallin [24, 25]. Among the above three mutants, the maximally affected and altered properties were observed in the recombinant αAN101D mutant [25]. Additionally, our recent results show that *in vitro,* the deamidated αA-and αB-crystallins facilitated greater

interaction with βA3-crystallin, leading to the formation of larger aggregates, which might contribute to the lens cataractogenic mechanism [46]. In the present study, the introduction of αAN101D trans-gene in a mouse model showed the following major *in vivo* effects in lenses of CYAAN101D- relative to CRYAAWT mice (not previously reported [28, 29]): (A) An age-related difference in protein profiles with an increasing association αAN101D with WI-protein fraction suggesting its insolubilization after 4-months of age. (B) The WS-HMW protein fraction showed a higher level of proteins with a greater M_r . (C) Mass spectrometric analysis showed preferential insolubilization of αA-, αB-, γD- and γE-crystallins, and nestin, which remained insoluble even in 8M urea. (D) The tight association of αAN101D with membranes relative to WTαA, which could not be fully dissociated with 8M urea treatment. (E) In vitro, αAN101D a showed greater affinity and binding to lens membranes relative WTαA. (F) The greater number of immunogold-labeled αAN101D relative WTαA binding to membrane along with relatively greater swelling of lens membranes, suggesting the potential water uptake due to intracellular ionic imbalance, and (G) The ionic imbalance was suggested by the greater Ca^{2+} uptake and 75% reduction in mRNA levels of Na, K-ATPase in the epithelial cells cultured from CRYAAN101D lenses relative to those from CRYAAWT lenses. Together, these findings suggest altered membrane integrity (possibly due to greater levels of αAN1010D binding to membrane than WTαA) resulting in intracellular ionic imbalance in CRYAAN101D lenses, which could play a major role in the cortical cataract development.

Among the lens crystallins, only α-crystallin show association with the membrane in both normal and cataractous lenses in several studies [6, 47-51]. Lens membranes contain both a high-affinity saturable and low-affinity non-saturable α-crystallin-binding sites [47, 51-53]. Alpha-crystallin binding to native membranes was enhanced on stripping of extrinsic proteins from the lens membrane surface to expose lipid moieties [32, 33], which contradicted a previous report that the crystallin mostly interacts with MP26 [54]. Even after stripping extrinsic membrane proteins by alkali-urea treatment, the full-length αA- and αB-crystallins remained associated with membranes of both bovine and human lenses [6]. Additionally, αB-crystallin showed three-fold higher binding to lens membrane relative to αA-crystallin, and their binding was affected by the residual membrane-associated proteins, suggesting that their binding behaviors were affected by an intrinsic lens peptide [6]. A large-scale association of proteins with cell membranes in the lens nucleus (mostly in the barrier region) occurs after middle age in human lenses [49], and such association was enhanced by mild thermal stress [50]. The *in vitro* studies further supported this because the binding capacity of α-crystallin from older lenses to lipids increased with age and decreased in diabetic donors who were treated with insulin [51]. This implied that under diabetic conditions, abnormal binding of α-crystallin to lens membrane occurred. Such information in the literature about membrane binding of native vs. post-translationally modified crystallins including the deamidated αAN101D species is presently lacking. Therefore, the results of the present study of relatively increased binding of αAN101D relative to WTαA are highly significant.

The RNA sequence and IPA data of our previous study [29] further support the findings of the present study. This study [29] showed that the genes belonging to gene expression, cellular assembly, and organization, and cell cycle and apoptosis networks were altered, and specifically, the tight junction-

signaling and Rho A signaling were among the top three canonical pathways that were affected in the CRYAAN101D lenses relative to CRYAA lenses. The present study showed an increased association of αAN101D to membrane, and this could lead to potential ionic imbalance affecting tight junction assembly and RhoA GTPase expression. This in turn causes increased proliferation and decreased of differentiation and denucleation of epithelial cells, and an accumulation of nuclei and nuclear debris in the lens anterior inner cortex and fiber cell degeneration. Some of these phenotypic changes could be cause or effects, but together could be responsible for the age-related cortical cataract development in CRYAAN101D lenses.

To maintain ionic balance within lens cells, a permeability barrier close to the surface of the lens is responsible for the continuous sodium extrusion via Na, K-ATPase-mediated active transport [35-37]. Without an active sodium extrusion, lens sodium and calcium contents are shown to increase resulting in lens swelling that leads to loss of lens transparency [35]. Similarly, an excessive intracellular Ca^{2+} levels can be detrimental to lens cells, and its increased levels play an important role in development of cortical cataract [37]. Therefore, homeostasis of Na^{+}, $K^{+,}$ Ca^{2+} and other ions within the lens has been recognized as of fundamental importance in lens pathophysiology. These have been altered as shown in our present and our previous study [29]. It is also possible that the increased Ca^{2+} levels could, in turn, leads to calpain activation and proteolysis of crystallins, which will be investigated in future.

Similar to our study, other studies have shown that an increased membrane binding of α- crystallin in the pathogenesis of many forms of cataracts. High molecular weight complexes (HMWCs) comprised of α-crystallin and other lens crystallins accumulate with aging and show a greater membrane binding capacity than native α-crystallin [51]. Other mutants of αA-crystallin, like the αAN101D mutant, also exhibit a greater membrane binding than corresponding wild-type species [55]. For example, in the αAR116C-associated congenital cataracts, an increased membrane binding capacity along with changes in complex polydispersity, and the reduction of subunit exchange were considered potential factors in the cataract pathogenesis [55]. Similarly, αA-crystallin R49C neo mutation influenced the architecture of lens fiber cell membranes and caused posterior and nuclear cataracts in mice [56].

Interactions between proteins and the cell membrane are an integral aspect of many biological processes, which are influenced by compositions of both membrane lipids and protein structure [57]. Reports have shown the age-related lipid compositional changes in the lens membrane, which might affect α-crystallin binding, i.e., in the nucleus of the human lenses, the levels of glycerophospholipids declined steadily by age 40 as opposed to the levels of ceramides and dihydroceramides increased approximately 100 fold during middle-age [58, 59]. Further, it has been shown that because of the elevation of sphingolipid levels with species, age, and cataract, lipid hydrocarbon chain order, or stiffness increased. Therefore, the increased membrane stiffness caused increase in light-scattering, reduced calcium pump activity, altered protein-lipid interactions, and perhaps slow fiber cell elongation [60]. Presently, whether similar changes occur in αAN101D lenses are not known.

Alpha A- and αB-crystallins differently associate with the cellular membrane, i.e. αA-crystallin may interact exclusively with membrane phospholipids, and thereby unaffected by the presence of extrinsic proteins on the membrane, whereas these proteins may act as conduits for αB-crystallin to bind to the membrane [59]. Presently, the specific binding mechanism of αAN101D to the membrane and age-related changes in lipid composition in lenses CRYAN101D vs. CRYAWT are unknown, and these are presently the focus of our investigations.

Conclusions

The results presented in this study suggest that an increased association of αAN101D relative WTαA with the lens membrane causes a possible loss of membrane integrity, leading to an ionic imbalance, and in turn to membrane swelling, cellular disorganization and finally cortical opacity. Our future study will determine the specific binding site in the αAN101D relative WTαA and changes in the membrane compositions that might facilitate the increased binding of the deamidated crystallin with the membrane.

Declarations

Ethics approval and consent to participate

No human subjects were involved in the study. All animal experiments were performed per protocols approved by the Institutional Animal Care and Use Committee (IACUC) of the University of Alabama at Birmingham (Protocol no. 130208393). Mice were housed in a pathogen-free environment at the facility of the University of Alabama at Birmingham.

Consent for publication

Not applicable

Availability of data and materials

All data generated or analyzed during this study are included in this published article [and its supplementary information files].

Competing interests

No competing interest

Funding

This study was funded by NIH grants, EY- 06400 (OS) and P30EY003039.

Authors' contributions

Kiran Srivastava and Dr. Roy Joseph conducted experiments, analyzed and interpreted the data and wrote the manuscript. Landon Wilson conducted the mass spectrometric analysis and analyzed and interpreted the results. Dr. Om Srivastava with the help of Dr. Roy Joseph analyzed and interpreted the data, and have written and edited the manuscript.

Source of Animals

The CRYAAN101D mouse model was generated by inserting the human lens αA-N101D transgene and the CRYAAWT mouse was generated by inserting human wild-type αA-transgene. Both mouse models were generated in Dr. Om Srivastava's laboratory. The details of the methodology are described in reference no. 28 (Gupta R, Asomugha CO, Srivastava OP. The common modification in αA-crystallin in the lens, N101D is associated with increased opacity in a mouse model. J Biol Chem. 2011; 286:11579-592)

Acknowledgements

Authors thank Ms. Rebecca Vance for the help with handling the CRYAAN101G and CRYAAWT mice. Thanks also goes to the High Resolution Imaging Facility, Targeted Metabolomics & Proteomics Laboratory and the Ocular Phenotyping and Molecular Analysis Core Facility of Vision Science Research Center at the University of Alabama at Birmingham

ARRIVE Guidelines

Minimum Standard of Reporting Checklist

Experimental design and statistics

The method section contains the information as described in the guideline.

Resources

The description of all the resources used are included in the Method section.

Availability of data and materials

All the data are available in the corresponding author's notebooks and his computer.

References

1. Mathias RT, TW White, X Gong. Lens gap junctions in growth, differentiation, and homeostasis. Physiol Rev. 2010;90:179-206.
2. Wride MA. Lens fibre cell differentiation, and organelle loss: many paths lead to clarity. Philosophical Transactions of the Royal Society of London B: Biol Sci. 2011; 366:1219-33.
3. Sharma KK, Santhoshkumar P. Lens aging: Effects of crystallins. Biochimica et Biophysica Acta-General Subjects. 2009;1790:1095-1108.

4. Stewart DN, Lango J, Nambiar KP, Falso MJS, FitzGerald PG, Rocke DM, Hammock BD, Buchholz BA. Carbon turnover in the water-soluble protein of the adult human lens. Mol Vis 2013;19:463-75.
5. Beebe DC, Holekamp NM, Siegfried C, Shui Y-Bo. Vitreoretinal influences on lens function and cataract. Philosophical Transactions of the Royal Society of London B: Biological Sciences 2011;366:1293-1300
6. Su S-P, McArthur JD, Friedrich MG, Truscott RJW, Aquilina JA. Understanding the α- crystallin cell membrane conjunction. Mol Vis, 2011;17:2798-2807.
7. Paterson CA, Delamere NA. ATPases and lens ion balance. Exp Eye Res, 2004;78:699- 703.
8. Vaghefi E, Beau P, Marc J, Donaldson P. Visualizing ocular lens fluid dynamics using MRI: manipulation of steady state water content and water fluxes. Am J Physiol-Reg, Integ Comp Physiol. 2011;301:R335-R342.
9. Borchman D, Yappert MC. Lipids and the ocular lens. J Lipid Res, 2010;51:2473-88.
10. Shiels A, Hejtmancik JF. *Chapter Twelve - Molecular Genetics of Cataract*, in *Progress in Molecular Biology and Translational Science*, J.F. Hejtmancik and M.N. John, Editors. 2015, Academic Press. p. 203-18.
11. Truscott RJW. Age-related nuclear cataract—oxidation is the key. Exp Eye Res, 2005;80:709-2512.
12. Harrington V, McCall S, Huynh S, Srivastava K, Srivastava OP. Crystallins in water soluble-high molecular weight protein fractions and water insoluble protein fractions in aging and cataractous human lenses. Mol Vis, 2004;10:476-89.
13. Harrington V, Srivastava OP, Kirk M. Proteomic analysis of water insoluble proteins from normal and cataractous human lenses. Mol Vis. 2007;13:1680-94.
14. Srivastava OP. Age-related increase in concentration and aggregation of degraded polypeptides in human lenses. Exp Eye Res. 1988;47:525-43.
15. Srivastava OP, McEntire JE, Srivastava K., Identification of a 9 kDa γ-crystallin fragment in human lenses. Exp Eye Res. 1992;54: 893-901.
16. Srivastava OP, Srivastava K, Silney C. Levels of crystallin fragments and identification of their origin in water soluble high molecular weight (HMW) proteins of human lenses. Curr Eye Res.1996:5:511-20.
17. Srivastava OP, Srivastava K. Degradation of γD- and γs-crystallins in human lenses. Biochem Biophys Res Commun. 1998;253:288-94.
18. Srivastava OP, Srivastava K, Harrington V. Age-related degradation of βA3/A1-crystallin in human lenses. Biochem Biophys Res Commun. 1999; 258:632-38.
19. Srivastava OP, Srivastava K. Existence of deamidated alpha B-crystallin fragments in normal and cataractous human lenses. Mol Vis. 2003;9:110-18.
20. Srivastava OP, Srivastava K. βB2-crystallin undergoes extensive truncation during aging in human lenses. Biochem Biophys Res Commun. 2003;31:44-49.

21. Srivastava OP, Srivastava K, Chaves JM, Gill AK. Post-translationally modified human lens crystallin fragments show aggregation in vitro, Biochem Biophys Rep. 2017;10:94-113.
22. Lampi KJ, Amyx KK, Ahmann P, Steel EA. Deamidation in human lens βB2-crystallin destabilizes the dimer. Biochemistry. 2006;45: 3146-53.
23. Wilmarth PA, Tanner S, Dasari S, Nagalla SR, Riviere MA, Bafna V, Pevzner PA, David LL. Age-related changes in human crystallins determined from comparative analysis of post-translational modifications in young and aged lens: Does deamidation contribute to crystallin insolubility? J Proteome Res. 2006;5:2554-66.
24. Gupta R, Srivastava OP. Deamidation affects structural and functional properties of human αA-crystallin and its oligomerization with αB-crystallin. J Biol Chem. 2004; 279: 44258-69.
25. Gupta R, Srivastava OP. Effect of deamidation of asparagine 146 on functional and structural properties of human lens αB-crystallin. Invest Ophthalmol Vis Sci. 2004;45: 206-14.
26. Rosenfeld L, Spector A. Changes in lipid distribution in the human lens with the development of cataract. Exp Eye Res. 1981; 6:641-650. 27. Harocopos GJ, Alvares KM, Kolker AE, Beebe DC, Human age-related cataract, and lens epithelial cell death. Invest Ophthalmol Vis Sci. 1998; 39:2696-2706.
27. Gupta R, Asomugha CO, Srivastava OP. The common modification in αA-crystallin in the lens, N101D is associated with increased opacity in a mouse model. J Biol Chem. 2011;286:11579-592.
28. Hegde SM, Srivastava K, Tiwary E, Srivastava OP. Molecular mechanism of formation of cortical opacity in CRYAAN101D transgenic mice cortical opacity in CRYAAN101D lenses. Invest Ophthalmol Vis Sci. 2014;55:6398-6408.
29. Wang Z, Han J, David LL, Schey KL. Proteomics and phosphoproteomics analysis of human lens fiber cell membranes. Invest Ophthalmol Vis Sci. 2013;54:1135-1143.
30. Tanaka M, Russell P, Smith S, Uga S, Kuwabara T, Kinoshita JH. Membrane alterations during cataract development in the Nakano mouse lens. Invest Ophthalmol Vis Sci.1980; 19:619-29.
31. Cobb BA, Petrash JM. Alpha-Crystallin chaperone-like activity and membrane binding in age-related cataracts. Biochemistry. 2002;41:483-490.
32. Cobb BA, Petrash JM. Characterization of α-crystallin-plasma membrane binding. J Biol Chem. 2000;275:6664-6672.
33. Laemmli UK. Cleavage of structural proteins during the assembly of the head of bacteriophage T4, Nature. 1970;227:680-685.
34. Delamere NA, Tamiya S. Lens ion transport: From basic concepts to regulation of Na, K-ATPase activity. Exp Eye Res. 2009;88:140-43.
35. Tseng SH, Tang MJ. Na,K-ATPase in lens epithelia from patients with senile cataracts. J Formosan Med Assoc. 1999;98:627-32.
36. Rhodes JD, Sanderson J. The mechanisms of calcium homeostasis and signalling in the lens. Exp Eye Res. 2009; 88:226-34.

37. Takata T, Oxford JT, Lampi KJ, Deamidation alters the structure and decreases the stability of human lens βA3-crystallin, Biochemistry. 2007, 46: 8861–8871.
38. Takata T, Oxford JT, Demeler B, Lampi KJ. Deamidation destabilizes and triggers aggregation of a lens protein, βA3-crystallin. Prot. Sci. 2008; 17:1565-1575.
39. Takemoto L, Boyle D. Deamidation of alpha-A crystallin from nuclei of cataractous and normal human lenses. Mol Vis. 1999;5:2.
40. Takemoto L, Boyle D. Deamidation of specific glutamine residues from alpha-A crystallin during aging of the human lens. Biochemistry. 1998;37:13681-685.
41. Haines PG, Truscott RJW. Age-dependent deamidation of lifelong proteins in the human lens, Invest Ophthalmol Vis Sc. 2010;51:3107-3114.
42. Srivastava OP, Srivastava K, Chaves JM, Gill AK. Post-translationally modified human lens crystallin fragments show aggregation in vitro, Bioche Biophys Rep. 2017;102:94- 131.
43. Santhoshkumar P, Udupa P, Murugesan R, Sharma KK. Significance of interactions of low molecular weight crystallin fragments in lens aging and cataract formation. J Biol Chem. 2008;283:8477-485.
44. Srivastava K, Chaves JM, Srivastava OP, Kirk M. Multi-crystallin complexes exist in the water-soluble high molecular weight protein fractions of aging normal and cataractous human lenses. Exp Eye Res. 2008;87:356-366
45. Tiwary E, Hegde S, Srivastava O. Interaction of βA3-crystallin with deamidated mutants of αA- and αB-crystallins. PLoS ONE, 2015, e0144621.
46. Chandrasekher G, Cenedella RJ. Properties of α-crystallin bound to lens membrane: Probing organization at themembrane surface. Exp Eye Res. 1997;64:423-30. 48.
47. Boyle DL, Takemoto L. EM immunolocalization of α-crystallins: Association with the plasma membrane from normal and cataractous human lenses. Cur Eye Res. 1996;15: 577-82.
48. Friedrich MG, Truscott RJW. Membrane association of proteins in the aging human lens: Profound changes take place in the fifth decade of life. Invest Ophthalmol Vis Sci. 2009;50:4786-93.
49. Friedrich MG, Truscott RJW. Large-scale binding of α-crystallin to cell membranes of aged normal human lenses: A phenomenon that can be induced by mild thermal stress. Invest Ophthalmol Vis Sci. 2010;51:5145-52.
50. Grami V, Marrero Y, Huang L, Tang D, Yappert MC, Borchman D. α-Crystallin binding in vitro to lipids from clear human lenses. Exp Eye Res. 2005;81:138-146.
51. Zhang WZ, Augusteyn RC. On the interaction of alpha-crystallin with membranes. Curr Eye Res. 1994;13:225-30.
52. Cenedella RJ, Chandrekher G. High capacity binding of alpha crystallins to various bovine lens membrane preparations. Curr Eye Res. 1993;11:1025-1038.
53. Mulders JWM, E Wojcik, H Blomendal. WW De Jong, Loss of high-affinity membrane binding of bovine nuclear α-crystallin. Exp Eye Res, 1989;49:149-52.

54. Cobb BA, Petrash JM, Structural and Functional Changes in the αA-Crystallin R116C Mutant in Hereditary Cataracts, Biochemistry, 2000, 39: 15791-15798.

55. Andley UP. αA-crystallin R49Cneomutation influences the architecture of lens fiber cell membranes and causes posterior and nuclear cataracts in mice. BMC Ophthalmology. 2009;9:1-11.

56. Watkins EB, Miller CE, Majewski J, Kuhl TL. Membrane texture induced by specific protein binding and receptor clustering: active roles for lipids in cellular function. Proc Nat Acad Sci (USA). 2011;108:6975-6980.

57. Hughes J, Deeley J, Blanksby SJ, Leisch F, Ellis S, Truscott RJW, Mitchell T. Instability of the cellular lipidome with age. AGE. 2012;34:935-47.

58. Huang L, Grami V, Marrero Y, Tang D, Yappert MC, Rasi V, Bourchman D. Human lens phospholipid changes with age and cataract. Invest Ophthalmol Vis Sci. 2005;46*:* 1682-89.

Supplemental File Legends

Supplemental Tables 1 to 4:

(A) Table 1: Water Insoluble-Urea Soluble (WI-US)-Protein Fraction of Alpha A-WT lenses.

(B) Table 2: Water Insoluble-Urea Insoluble (WI-UI)-Protein Fraction of AlphaA N101D lens

(C) Table 3: Water insoluble-urea soluble alphaAN101D (Mr >30 kDa)

(D) Table 4: Water insoluble-urea insoluble alpha A N101D (Mr >30 kDa)

Figures

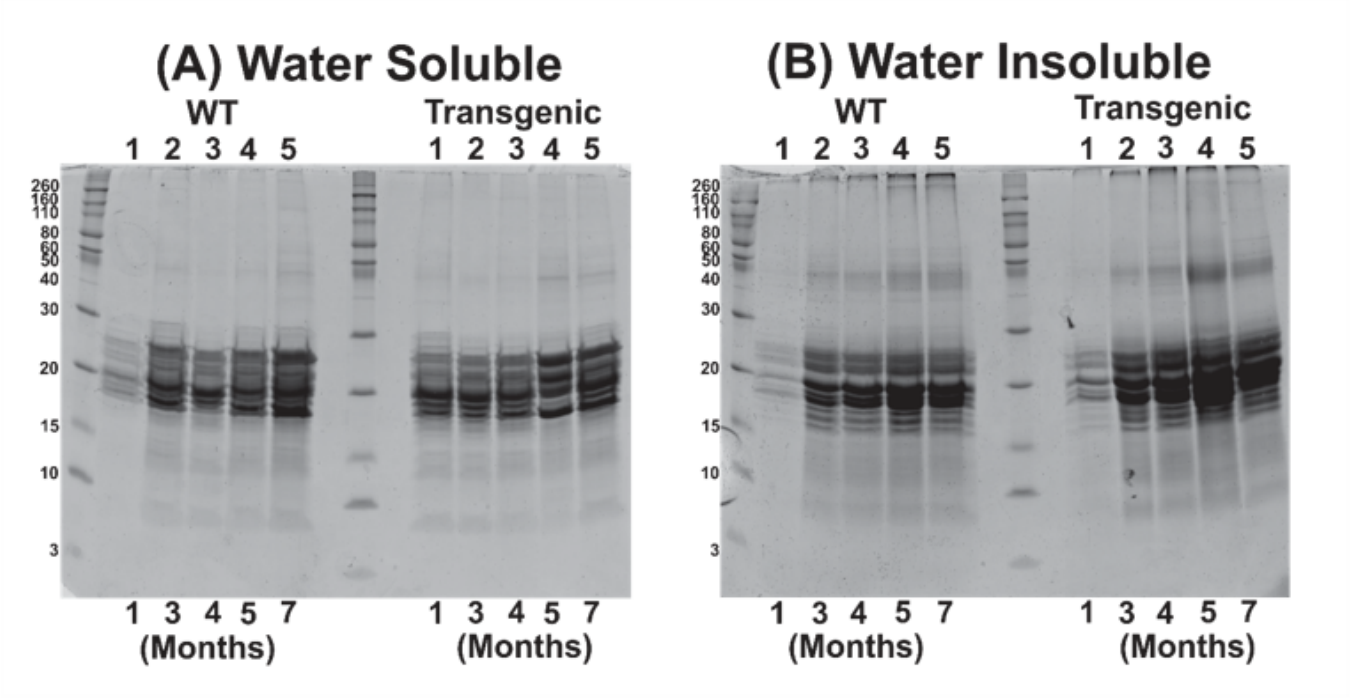

Figure 1

Table: Age-related changes in protein distribution in water soluble and water insoluble fractions In lenses of WT and αAN101D mice.

Age (Months)	Wild type (mg) WS	WI	αAN101D (mg) WS	WI	Percent insoluble of total protein WT	N101D
1	0.96	0.108	1.07	0.57	10.1	34.7
3	1.8	1.14	1.16	0.68	38.7	36.9
4	1.43	1.27	1.47	2.0	47.03	54.05
5	1.69	1.15	1.5	2.2	40.5	59.4
7	1.74	1.9	1.74	2.2	52.1	55.8

Figure 1

SDS-PAGE analysis of WS- and WI-proteins from lenses of different aged from CRYAAWT- and CRYAAN101D mice. The WS- and WI-proteins were isolated under identical conditions and with identical volumes of buffers (See Methods) from two lenses of mice of ages as shown at the bottom of gels (A) and (B). Note that a greater insolubilization and aggregated proteins (Mr >30 kDa) were seen in WI-proteins of lenses of 4-month and older CRYAAN101D mice compared to age-matched lenses from CRYAAWT mice. The table shows quantification of protein levels in the WS- and WI-protein fractions of lenses of different ages from CRYAAN101D and CRYAAWT mice.

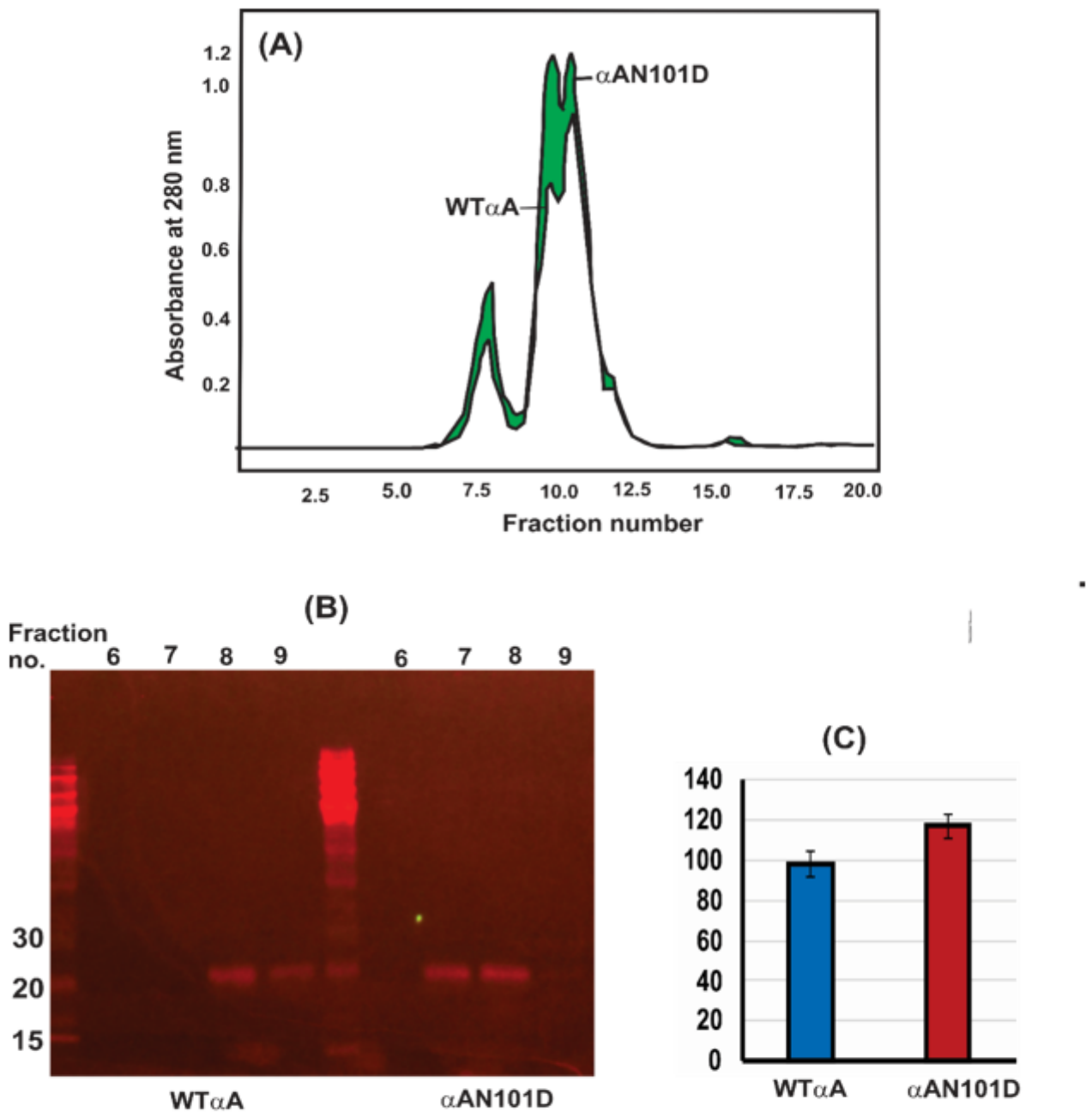

Figure 2

Figure 2

Size-exclusion HPLC (using a G-4000PWXL column) and SDS-PAGE analysis of WS-HMW proteins eluted in the void volume. (A) HPLC-protein elution profiles at 280 nm of WS-proteins from lenses of 5-month-old CRYAAN101D- and CRYAAWT mice. The green region shows the difference in the A280 profiles of WS-proteins from the two type of lenses. (B) Western blot analysis of the void volume peaks (constituted by the fraction no. 6 to 9 in [A]) following HPLC separation of WS-proteins from lenses of CRYAAN101D- and

CRYAAWT mice. Note that in the CRYAAWT lenses, the αA-immunoreactive bands were in fractions no. 8 and 9 whereas it were in fraction no. 7 and 8 in CRYAAN101D lenses, suggesting a higher Mr of HMW proteins in the latter.

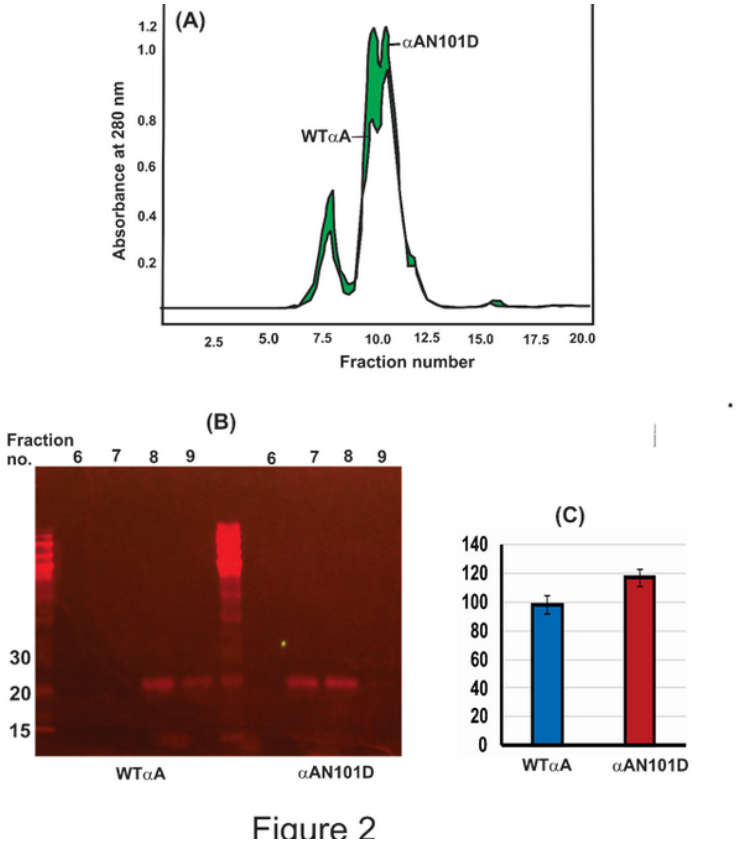

Figure 2

Figure 3

SDS-PAGE analysis of WI-US- and WI-UI-protein fractions of 5-month-old lenses from CRYAAN101D and CRYAAWT mice. To normalize the protein analyses, the protein fractions were isolated under identical conditions and with identical buffer volumes. Equal volumes of protein fractions from lenses of two types of mice were used during the analysis. The four fractions numbers as 1 to 4 (containing total proteins in WI-US- and WI-UI-fractions) and four fractions numbered as a to d (containing aggregated proteins with Mr >30 kDa) were analyzed by mass-spectrometric methods, and the results are shown in supplemental Tables 1 to 4.

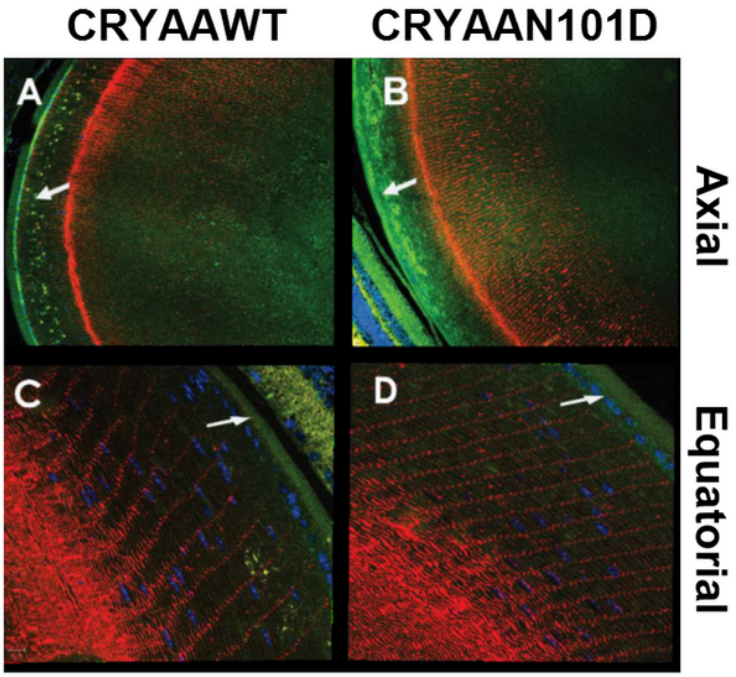

Figure 4

Figure 4

Immunohistochemical and transmission electron microscopic analyses of lens sections. (A) Confocal-immunohistochemical analysis of 5-month old lenses from CRYAAN101D and CRYAAWT mice by using anti-His monoclonal (green, for □A detection)- and polyclonal anti-aquaporin 0 (red, for membrane detection)-antibodies. A and B: The axial sections at 10X magnification showed an irregular deposition of His-tagged □A (Green) in the lens outer cortex of CRYAAN101D mice (in B, shown by an arrow) relative to CRYAANWT mice (in A, shown by an arrow). The equatorial sections (at 40X magnification) show a greater deposit of green fluorescence in the outer cortex of CRYAAN101D lens relative to CRYAAN WT lens (shown by arrows in Figure 4C and D).

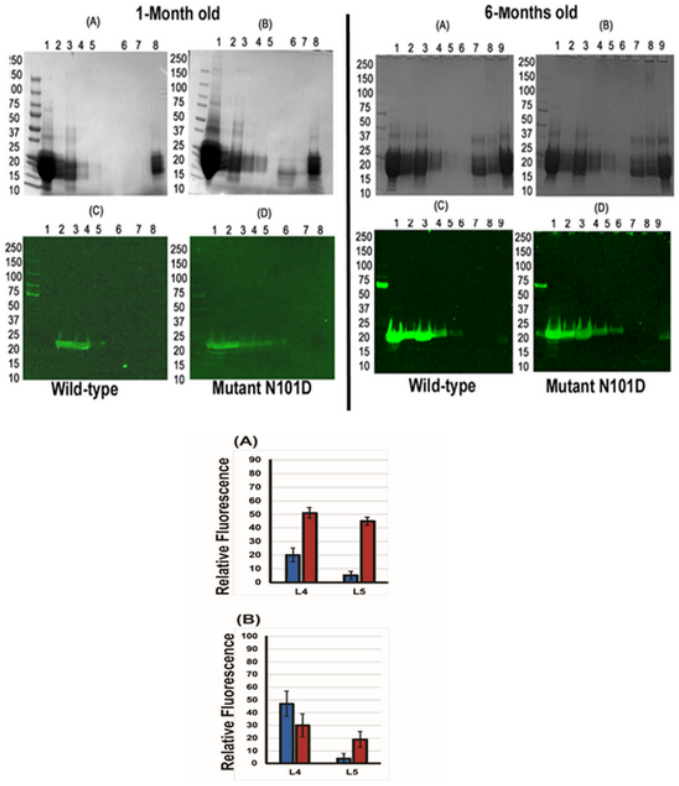

Figure 5

Figure 5

Upper Panels (A) and (B): The relative levels of association of WTαA and αAN101D with the purified membrane preparations at different membrane purification steps. During the Western blot, analysis anti-His- and anti-aquaporin 0-antibodies were used. The results of relative levels of His-tagged αA (green fluorescence) in lenses of 1-month old lenses (Figure left panel, WTαA [A and C] and αAN101D [B and C]) and 6-month old lenses (right panel, WTαA [A and C] and αAN101D [B and D] are shown. In both left and right top panels in (A) and (B) show Coomassie blue-stained protein bands and C and D show western blot immunoreactivity with anti-His antibody. Additionally, in both left and right panels, the lanes 1, 2 and 3 show the WS-protein fractions recovered after 1st, 2nd and 3rd consecutive washes in buffer B to solubilize WS-proteins, respectively. Lanes 4 and 5 represent the urea soluble-protein fractions recovered during two consecutive washes of WI-protein pellet with buffer B containing 8M urea, Lower Panels (A) and (B): Quantification of immunoreactive bands of αA recovered in urea-soluble fractions (Lane 4 [L4] and lane 5 [L5] represent two consecutive urea wash of WI proteins during membrane isolation from lenses of CRYAAWT and CRYAAN101D mice as shown in Western blot analysis in Figure 5. (A) Relative levels of immunoreactive WTαA lenses (blue) and αA-N101D αA (red) during membrane purification from 1-month old lenses. (B) Relative levels of immunoreactive WTαA lenses (blue) and αA-N101D αA (red) during membrane purification from 6-months old lenses. Note that relatively higher levels of αA-N101D than WTαA was associated with purified membranes in lanes 4 (in 1-month old) and lane 5 (in both 1- and 6- month-old) of the two types of lenses.

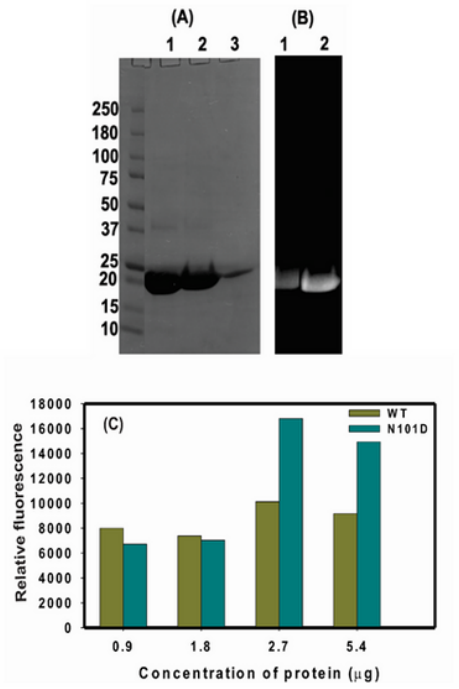

Figure 6

Figure 6

Relative in vitro binding of recombinant ΔAN101D and WTΔA proteins to lens membrane. (A) The recombinant WT ΔA- and ΔA-N101D proteins were labeled with Alexa 350, purified by a size-exclusion HPLC column and analyzed by SDS-PAGE. Lane 1: Coomassie blue-stained WTΔA, lane 2: ΔA-N101D mutant protein, and lane 3: purified lens membrane from non-transgenic C57 mice. (B) Images of labeled ΔAN101D and WTΔA proteins. Lane 1: Alexa 350-labeled WT ΔA, and lane 2: ΔA-N101D protein. (C) Binding of a WT ΔA, and ΔA-N101D with purified lens membrane (2.5 mg protein; isolated from 1- to 3-month old non-transgenic C57 mice). During the binding assay, the protein mixtures were incubated with increasing but identical concentrations of either Alexa-labelled WTΔA- or ΔA-N101D at 37oC for 6 h, centrifuged at 14,000Xg and the supernatant and pellet (membrane fraction) recovered. After washing the membrane fraction with water and centrifugation as above, the relative fluorescence of membranes incubated with WT ΔA- and ΔA-N101D mutant proteins was determined. The values reported are the average of triplicate assays.

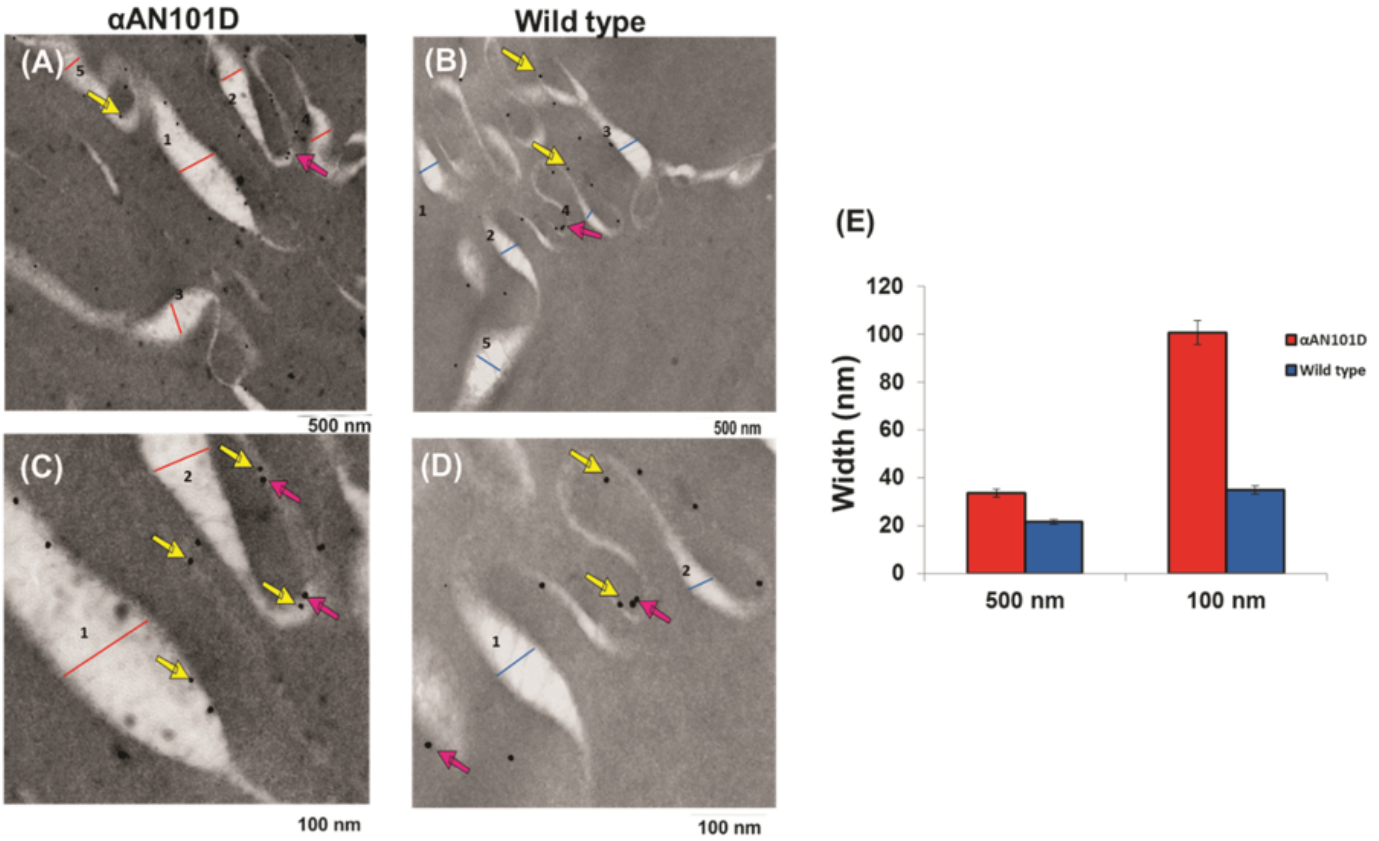

Figure 8

Figure 7

Immunogold-labeling to determine relative localization of αA-WT and αA-N101D in lens membranes of CRAAN101D and CRAAWT mice. (A) and (C) show membranes of lenses from CRYAAN101D (at 500 nm magnification) and (B) and (D) from CRYAAWT (at 100 nm and magnification). The bigger particles (25 nm, red arrows) represented the aquaporin 0 whereas the smaller gold particles (10 nm, yellow arrows) represented the His-tagged αAN101D and WT αA. As shown in the representative images in (A) to (D), both 10 nm and the 20 nm gold particles were bound to membranes. (E): Quantification of width of membranes from lenses of CRAAN101D and CRAAWT mice. Note that the lens membranes of CRAAN101D mice were about 1.5X (at 500 nm magnification) and 3X (at 100 nm magnification) wider that those from CRAAN101D mice, suggesting membrane swelling of the former lenses.

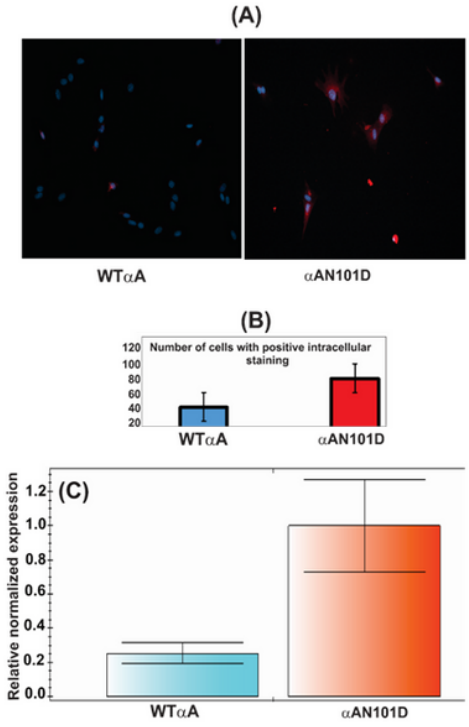

Figure 8

Figure 8

Determination of levels of intracellular Ca2+ and Na, K-ATPase mRNA in cultured epithelial cells from lenses of CRAAN101D and CRAAWT mice. (A) Left and right panels show intracellular Ca2+ staining following uptake from calcium orange in cells from CRAAWT- and CRAAN101D mice, respectively. (B) Quantification by Image J of the number of cells that showed positive intracellular Ca2+-staining following uptake from calcium orange in CRAAWT- and CRAAN101D cells. (C) Relative levels of Na, K-ATPase mRNA in epithelial cells from CRAAWT- and CRAAN101D mice as determined by the QRT-PCR method.